

Special  
Issue

# Carbon Dioxide Hydrogenation to Formate Catalyzed by a Neutral, Coordinatively Saturated Tris-Carbonyl Mn(I)-PNP Pincer-Type Complex

Sylvia Kostera,<sup>[a]</sup> Gabriele Manca,<sup>[a]</sup> and Luca Gonsalvi<sup>\*[a]</sup>

CO<sub>2</sub> catalytic hydrogenation to formate was achieved (TON<sub>max</sub> = ca. 3800) in the presence of the neutral, halide-free, coordinatively saturated tris(carbonyl) manganese pincer-type complex [Mn(PNP)(CO)<sub>3</sub>], bearing a diarylamido pincer-type PNP ligand, using DBU as base and LiOTf as Lewis acid additive, under mild

reaction conditions (60 bar, 80 °C). DFT calculations suggest that the precatalyst activation key step occurs by intermolecular, base assisted dihydrogen heterolytic splitting rather than by the expected ligand-assisted intramolecular MLC-type mechanism.

## Introduction

The growth in concentration of carbon dioxide (CO<sub>2</sub>) in the atmosphere has reached alarming levels.<sup>[1]</sup> Scientists worldwide are developing technologies to reduce CO<sub>2</sub> emissions, for example using Carbon Capture, Utilization and Storage (CCUS) methods. Chemists have used CO<sub>2</sub> for many years as an abundant source for C-1 syntheses, using catalytic processes to overcome the thermodynamic stability of this inert molecule, to obtain value-added products such as formic acid (HCO<sub>2</sub>H), formaldehyde (HCHO), methanol (CH<sub>3</sub>OH), dimethyl ether (CH<sub>3</sub>OCH<sub>3</sub>), methane (CH<sub>4</sub>) or higher hydrocarbons through reduction methods.<sup>[2]</sup> Formic acid, the simplest product derived from the 2-electrons CO<sub>2</sub> reduction or direct hydrogenation,<sup>[3]</sup> currently has a large market for applications, which justifies more investigation for its sustainable synthesis from CO<sub>2</sub>.

The homogeneous hydrogenation of CO<sub>2</sub> to formic acid and/or formate salts in the presence of noble and non-noble transition metal complexes is nowadays a mature science,<sup>[2c,4]</sup> and the use of cheap earth-abundant transition metal complexes is rapidly growing in interest. Manganese, the third most abundant metal in the Earth's crust, has recently been used in homogeneous catalytic processes such as hydrogenation, dehydrogenation, and hydroelementation reactions with various substrates.<sup>[5]</sup> Interestingly, only few manganese catalysts

have been reported to date for CO<sub>2</sub> hydrogenation to formates (Figure 1).

The first example of Mn(I)-catalyzed hydrogenation of CO<sub>2</sub> to formate was reported as a result of our collaboration with Kirchner's group in 2017.<sup>[6]</sup> The process was carried out in the presence of the hydridocarbonyl complex [MnH(PNP<sup>NH</sup>-iPr)(CO)<sub>2</sub>], stabilized by a PN<sup>3</sup>P pincer-type ligand, at catalyst loadings in range of 0.1–10 μmol. Quantitative yields of formate and TONs (TON = turnover number) up to 10000 were obtained after 24 h using 1,8-diazabicycloundec-7-ene (DBU) as base, 80 bar H<sub>2</sub>/CO<sub>2</sub> (1:1) total pressure, 80 °C. Notably, the system was dramatically improved adding LiOTf (OTf = CF<sub>3</sub>SO<sub>3</sub><sup>-</sup>, triflate) as a co-catalyst, reaching TON > 30000. Proton-responsive, non-pincer type Mn(I)-bipyridyl complexes were used by Nervi, Khusnutdinova and coworkers in the same year. With an *o*-OH substituted ligand, formate was obtained in 98% yield after 24 h, reaching a maximum TON of 6250 using 0.015 mol% of catalyst, CH<sub>3</sub>CN as solvent, DBU, 60 bar H<sub>2</sub>/CO<sub>2</sub> (1:1), 65 °C.<sup>[7]</sup> Next, Mn(I) complexes bearing pyridyl-type PNN

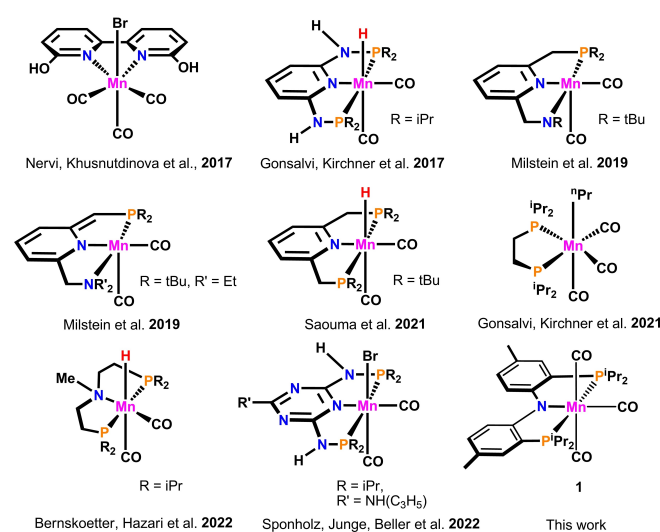


**Figure 1.** Mn(I) complexes used as catalysts for CO<sub>2</sub> hydrogenation to formate.

[a] Dr. S. Kostera, Dr. G. Manca, Dr. L. Gonsalvi  
Istituto di Chimica dei Composti Organometallici (ICCOM)  
Consiglio Nazionale delle Ricerche (CNR)  
Via Madonna del Piano 10, 50019 Sesto Fiorentino (Florence) (Italy)  
E-mail: luca.gonsalvi@cnr.it

Supporting information for this article is available on the WWW under <https://doi.org/10.1002/chem.202302642>

This manuscript is part of a joint special collection on Manganese Homogeneous Catalysis.

© 2023 The Authors. Chemistry - A European Journal published by Wiley-VCH GmbH. This is an open access article under the terms of the Creative Commons Attribution License, which permits use, distribution and reproduction in any medium, provided the original work is properly cited.

pincer ligands were studied by Milstein and coworkers. In the presence of a cheaper and milder base (KOH),  $\text{HCO}_2\text{K}$  was obtained in up to 23% yield with 10 mol% of catalyst, THF as solvent, 60 bar  $\text{H}_2/\text{CO}_2$  (1:1), 110 °C, 60 h.<sup>[8]</sup> A slightly modified system was then disclosed by Saouma and coworkers, using a pyridyl-type PNP complex and  $\text{KO}^t\text{Bu}$  as base, reaching TON = 58 after 18 h at 100 °C.<sup>[9]</sup> In 2022, Bernskoetter, Hazari and coworkers demonstrated the use of a PNP-type Mn-MACHO complex {MACHO = Bis[2-(diisopropylphosphino)ethyl]methylamine}, obtaining a rewarding TON = 18300 with DBU, LiOTf, 70 bar  $\text{H}_2/\text{CO}_2$  (1:1), 80 °C, 24 h.<sup>[10]</sup> In the same year, Sponholz, Junge, Beller and coworkers studied the use of  $\text{PN}^5\text{P}$ -type Mn(I) pincer complexes, with a triazole ligand core instead of pyridine, for this process. An outstanding efficiency (92% yield, TON = 230000) was achieved using lysine or potassium lysinate as base, 80 bar  $\text{CO}_2/\text{H}_2$  (1:3),  $\text{H}_2\text{O}/\text{THF}$  (1:1), 115 °C.<sup>[11]</sup> The year before, in a collaborative study with Kirchner and coworkers, we explored the use of a simple textbook bis(phosphine)-Mn(I) alkylcarbonyl complex  $[\text{Mn}(\text{CH}_2\text{CH}_2\text{CH}_3)(\text{dippe})(\text{CO})_3]$ , in an effort to achieve ligand simplification. The catalytic tests were run under mild conditions [75 bar  $\text{CO}_2/\text{H}_2$  (1:3), 80 °C], in the presence of DBU and LiOTf. Formate was obtained in >98% yield after 24 h, reaching a maximum TON of 1988 with 2  $\mu\text{mol}$  of catalyst in THF.<sup>[12]</sup>

The literature data summarized above clearly show a preference for pincer-type complexes in Mn-catalyzed  $\text{CO}_2$  hydrogenation. The common features of these precatalysts are the presence of a tridentate pincer ligand, forcing meridional coordination to the Mn center, two CO ligands and either a bromide or hydride ligand to saturate the octahedral coordination sphere. Bromide is a good leaving group and can be easily exchanged *in situ* with hydride in presence of base and hydrogen, to give a Mn–H active species interacting with  $\text{CO}_2$  to generate a  $\kappa^1\text{-H}$ -formate species. In pyridine- or amine-based PNP complexes, the pincer ligands often participate in substrate activation, via metal-ligand cooperation (MLC) mechanisms involving either dearomatization/aromatization or protonation/deprotonation steps.<sup>[13]</sup> On the other hand, in Mn(I) bis(phosphine) catalysts,<sup>[12]</sup> the ligand cannot activate a MLC mechanism, and the active pentacoordinate species  $[\text{MnH}(\text{dippe})(\text{CO})_2]$ , that activates  $\text{CO}_2$  by an inner-sphere mechanism, was obtained by elimination of butanal under a pressure of hydrogen. Thus, either the presence of a hydride ligand, or the possibility to easily generate a vacant coordination site by CO elimination, seem to be required to achieve catalytic activity with these classes of Mn(I) complexes.

Following on our interest in the fundamental aspects of this field of research, we decided to explore the applicability of coordinatively saturated Mn(I) pincer-type complexes bearing three CO coligands in  $\text{CO}_2$  hydrogenation and to pinpoint the mechanistic details of the catalytic reaction. Although the use of cationic Mn(I) tris(carbonyl) pincer-type complexes has been demonstrated, for example in catalytic ketone hydrogenation,<sup>[14]</sup> to the best of our knowledge no example of use of this class of complexes, especially neutral halide-free analogues, has been reported so far in the literature for this kind of process. By a perusal of the available literature, we identified complex  $[\text{Mn}$

(PNP)(CO)<sub>3</sub>] (1), stabilized by a diarylamido PNP-pincer ligand, *i.e.* the deprotonated form of bis(2-(diisopropylphosphino)-4-methylphenyl)amine, as a suitable candidate for investigation. This compound belongs to a class of PNP ligands that has been studied in particular by Ozerov and coworkers.<sup>[15]</sup> In complex 1, the PNP ligand is negatively charged, giving a formal Mn–N amido bond that can in principle facilitate intramolecular hydrogen activation via a MLC mechanism. The complex was tested as catalyst for  $\text{CO}_2$  hydrogenation under various conditions of  $\text{H}_2/\text{CO}_2$  gas ratios and pressures, solvents, catalyst concentrations, with or without the addition of a Lewis acid (LiOTf, *vide infra*). By a combination of NMR experiments and DFT calculations, it was possible to clarify mechanistic details and propose a plausible catalytic mechanism. The results of this study are hereby described.

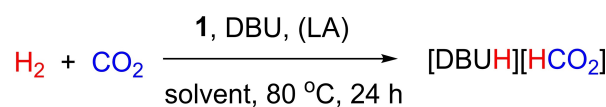
## Results and Discussion

### Catalytic tests

Complex 1 was synthesized using one of the methods described by Ozerov, Nocera and coworkers in 2009,<sup>[16]</sup> namely by reaction of neutral bis(2-(diisopropylphosphino)-4-methylphenyl)amine with 0.5 equiv. of  $\text{Mn}_2(\text{CO})_{10}$  in refluxing hexamethyldisiloxane. <sup>1</sup>H, <sup>31</sup>P{<sup>1</sup>H} and FTIR characterization of the product obtained as an orange powder were in agreement with the original data.  $\text{CO}_2$  hydrogenation tests (Scheme 1) were initially carried out in the presence of 1 under the conditions previously applied with  $[\text{Mn}(\text{CH}_2\text{CH}_2\text{CH}_3)(\text{dippe})(\text{CO})_3]$ , *i.e.* using DBU as base (1000 equiv. to 1), under  $\text{H}_2/\text{CO}_2$  (1:1) 60 bar total pressure, at 80 °C for 24 h.<sup>[11]</sup>

In the first screening of reaction parameters, the choice of best solvent was assessed. Using dry THF as solvent and a 1/DBU ratio of 1:1000, formate was obtained in 77% yield with respect to DBU, with a corresponding TON = 777. By changing the solvent to a THF/ $\text{H}_2\text{O}$  mixture (10:1),<sup>[6]</sup> no formate was obtained at the end of the reaction. The reason of adverse effect of added water is unclear, perhaps due to catalyst decomposition, witnessed by a dark colored solution observed at the end of the reaction. By using toluene, only 5% yield in formate was observed. In this solvent, complex 1 resulted only partially soluble. Based on these results, dry THF was chosen as solvent for the rest of the study.

Next, the effect of 1/DBU ratio was tested, in the absence or presence of a Lewis acid (LA), at different ratios 1/LA (Table 1), under the same conditions of pressure, temperature and reaction time (60 bar total pressure, 80 °C, 24 h). As explained by Bernskoetter and Hazari in an excellent review article, the effect of Lewis acids in reversible  $\text{CO}_2$  hydrogenation is to favor



**Scheme 1.**  $\text{CO}_2$  hydrogenation to formate in the presence of 1 and DBU, with or without addition of a Lewis acid (LA) co-catalyst.

**Table 1.** Screening of the effects of catalyst/base/additive ratios in catalytic CO<sub>2</sub> hydrogenation with **1**, with or without LiOTf co-catalyst.

Entry	1/DBU	1/LiOTf	LiOTf/DBU	TON <sup>[a]</sup>	Yield <sup>[b]</sup> (%)
1	1/1000	–	–	777	77
2	1/2000	–	–	561	28
3	1/1000	1/100	1/10	1004	>99
4	1/2000	1/50	1/20	907	46
5	1/2000	1/100	1/40	1099	55
6	1/2000	1/200	1/10	1290	65
7	1/5000	1/500	1/10	2863	57
8 <sup>[c]</sup>	1/5000	1/500	1/10	2285	46
9 <sup>[d]</sup>	1/5000	1/500	1/10	2240	45
10 <sup>[e]</sup>	1/5000	1/500	1/10	3805	76
11	1/10000	1/1000	1/10	921	9

Reaction conditions: catalyst **1**, 1–10 μmol; DBU, 10 mmol; LiOTf = 0.25–1 mmol; THF, 5.5 mL; 60 bar total pressure H<sub>2</sub>/CO<sub>2</sub> (1:1); 80 °C; 24 h. [a] TON = (mmol formate)/(mmol catalyst). [b] Yield = [(mmol formate)/(mmol DBU)] × 100. The amount of formate was calculated from the integration of the corresponding <sup>1</sup>H NMR signal in D<sub>2</sub>O against an internal standard (DMF). [c] 80 bar total pressure H<sub>2</sub>/CO<sub>2</sub> (1:1). [d] 100 °C. [e] Reaction time: 72 h. All experiments were repeated at least twice to check for reproducibility, average error ca. 6%.

more accessible transition states, especially in combination with pincer-type complexes of base metals.<sup>[17]</sup> In keeping with our previously published results,<sup>[6,11]</sup> LiOTf was chosen as a suitable LA to promote CO<sub>2</sub> hydrogenation to formate, using 60 bar total pressure of a H<sub>2</sub>/CO<sub>2</sub> = 1:1 gas mixture and a 1/DBU in different ratios.

Without LiOTf, the initial test (Table 1, entry 1) was repeated using a 1/DBU ratio of 1:2000. A decrease in activity was observed, with a maximum TON of 561 and a yield of 28% in formate (entry 2). In the presence of LiOTf (1 mmol, 1/LiOTf = 1:100), formate was obtained in >99% yield (TON = 1004, entry 3). The 1/LiOTf ratio was then varied in three different runs (entries 4–6), maintaining a 1/DBU ratio of 1:2000. Under these conditions, the best TON = 1290 was obtained at 1/LiOTf = 1:200 (entry 6). By further optimization, an even higher TON = 2863 was obtained by lowering the 1/DBU ratio to 1:5000, using a 1/LiOTf ratio of 1:500 (entry 7). Slightly lower TON values were measured using 1/DBU = 1:5000, 1/LiOTf = 1:500 at higher pressure (80 bar, 60 °C, TON = 2240, entry 8) or higher temperature (100 °C, 60 bar, TON = 2285, entry 9). At longer reaction time (72 h, entry 10), using 1/DBU = 1:5000, 1/LiOTf = 1:500, 60 bar, 80 °C, it was possible to increase further the yields up to 76%, corresponding to a maximum TON of 3805. On the other hand, lowering the 1/DBU ratio to 1:10000, with a LiOTf/DBU ratio of 1:10, 60 bar, 80 °C, 24 h, gave formate in only 9% yield, with TON = 921 (entry 11).

In previous studies,<sup>[11,12]</sup> it was demonstrated that an increase of the H<sub>2</sub>/CO<sub>2</sub> ratio can be beneficial in Mn(I)-catalyzed CO<sub>2</sub> hydrogenation. To verify whether tuning this parameter could further improve the activity, catalytic tests using 1/DBU = 1:2000, 1/LiOTf = 1:200, 80 °C, were run for 24 h at H<sub>2</sub>/CO<sub>2</sub> ratios of 2:1 (75 bar total pressure) and 9:1 (100 bar total

pressure). Small amounts or traces of formate were observed in both cases (Table 2, entries 2 and 3), accompanied by formation of dark brown colored solutions at the end of the reactions, indicative of catalyst decomposition. Thus, it was confirmed that a 1:1 ratio of gases should be preferred for this catalytic system (Table 2, entry 1).

Finally, in order to rule out catalytic activity due to the metal precursor or to the free ligand, additional tests were run (Table 3) and the results were compared with those obtained with preformed **1**. Only traces of formate were observed after 24 h, confirming that the well-defined complex **1** is required as precatalyst for CO<sub>2</sub> hydrogenation.

### Mechanistic studies

In order to establish mechanistic details on the formation of the catalytic active species and on substrates activation leading to formate, NMR experiments and DFT calculations were carried out. We reasoned that activation of precatalyst **1** might occur under catalytic conditions, either by dissociation of one CO ligand or through ligand (reversible) hemilability, to free a coordination site from the hexacoordinate metal center. In this way, the resulting pentacoordinate species may favor hydrogen splitting and form a Mn–H moiety able to interact with CO<sub>2</sub>, as described in the literature for related Mn(I) pincer-type

**Table 2.** Catalytic CO<sub>2</sub> hydrogenation with **1** using different H<sub>2</sub>/CO<sub>2</sub> partial pressure ratios.

Entry	pH <sub>2</sub> /pCO <sub>2</sub> (bar)	1/LiOTf	LiOTf/DBU	TON <sup>[a]</sup>	Yield <sup>[b]</sup> (%)
1	30/30	1/200	1/10	1290	65
2	50/25	1/200	1/10	65	1
3	90/10	1/200	1/10	16	< 1

Reaction conditions: catalyst **1**, 5 μmol; DBU, 10 mmol; LiOTf, 1 mmol; THF, 5.5 mL; H<sub>2</sub>/CO<sub>2</sub>, 1:1, 2:1 or 9:1 ratios, partial pressures as indicated; 80 °C, 24 h. [a] TON = (mmol formate)/(mmol catalyst). [b] Yield = [(mmol formate)/(mmol DBU)] × 100. The amount of formate was calculated from the integration of the corresponding <sup>1</sup>H NMR signal in D<sub>2</sub>O against an internal standard (DMF). All experiments were repeated at least twice to check for reproducibility, average error ca. 6%.

**Table 3.** Catalytic CO<sub>2</sub> hydrogenation with **1**, metal precursor Mn<sub>2</sub>(CO)<sub>10</sub> and free PNP ligand.

Entry	Catalyst	1/LiOTf	LiOTf/DBU	TON <sup>[a]</sup>	Yield <sup>[b]</sup> (%)
1	<b>1</b>	1/100	1/10	1004	>99
2	Mn <sub>2</sub> (CO) <sub>10</sub>	1/100	1/10	26	1
3	PNP ligand	1/100	1/10	4	< 1

Reaction conditions: catalyst: 10 μmol; DBU, 10 mmol; LiOTf, 1 mmol; THF, 5.5 mL; H<sub>2</sub>/CO<sub>2</sub> (1:1) pressure; 80 °C, 24 h. [a] TON = (mmol formate)/(mmol catalyst); [b] Yield = [(mmol formate)/(mmol DBU)] × 100. The amount of formate was calculated from the integration of the corresponding <sup>1</sup>H NMR signal in D<sub>2</sub>O against an internal standard (DMF). All experiments were repeated at least twice to check for reproducibility, average error ca. 6%.

complexes.<sup>[18]</sup> In their original article,<sup>[16]</sup> Ozerov, Nocera and coworkers reported that mixtures of **1** and pentacoordinate [Mn(PNP)(CO)<sub>2</sub>] (**2**) derived by elimination of one CO ligand from the metal coordination sphere, could be obtained either by refluxing **1** in mesitylene for 6 h, or by reaction of **1** with [(*p*-cymene)RuCl<sub>2</sub>]<sub>2</sub> in fluorobenzene at 60 °C for 3 days. Complex **2** was identified by <sup>31</sup>P{<sup>1</sup>H} NMR in C<sub>6</sub>D<sub>6</sub>, as a singlet at 83.0 ppm and by solution IR spectra (C<sub>6</sub>D<sub>6</sub>), showing two νCO bands at 1900 (s) and 1838 (s) cm<sup>-1</sup>.

In our study, the <sup>31</sup>P{<sup>1</sup>H} NMR analysis of the reaction mixtures at the end of the typical catalytic runs in the presence of **1** invariably showed the presence of a single species characterized by a broad singlet at ca. 84 ppm, due to **1**. Our attempts to synthesize **2** by reaction of **1** with Me<sub>3</sub>NO, a common method often used in organometallic chemistry to achieve selective decarboxylation,<sup>[19]</sup> unfortunately were not successful even under prolonged reflux conditions in various solvents, and either unreacted **1** or extensive decomposition were observed at the end of the reactions.

Two additional experiments were carried out to verify the formation of the putative Mn-hydrido complex [MnH(PNP)(CO)<sub>2</sub>] (**3**) by exposing **1** to a hydrogen pressure (20 bar), in the presence and absence of base, at 25 °C for 4 days. The experiments were inconclusive, and the corresponding <sup>1</sup>H NMR spectra did not show signals at negative chemical shift values, as expected for the formation of Mn–H bonds.

DFT calculations were then run to examine the energy requirements and propose a possible reaction pathway for the catalytic system. Initially, the analysis of the electronic structure of the optimized compound **1** was carried out by using Gaussian 16 software<sup>[20]</sup> at PBE1PBE-DFT level of theory<sup>[21]</sup> with the inclusion of the dispersion forces contribution. More details on the computational method are described in the Supporting Information. The Highest Occupied Molecular Orbital (HOMO) was found to be delocalized over the PNP anionic ligand with only a contribution of 28% from the nitrogen atom, as shown in Figure 2, suggesting a weak nucleophilic character of the amido-type ligand. For this reason, a potential involvement of this atom in H<sub>2</sub> activation by heterolytic splitting seems unlikely.

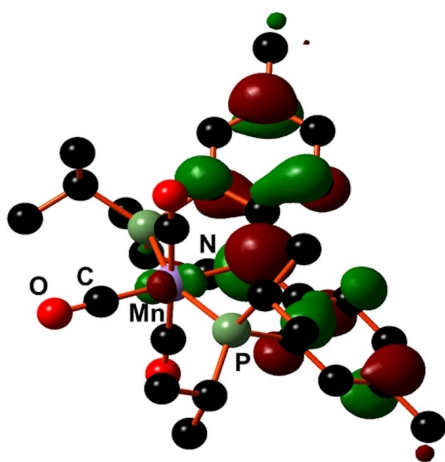


Figure 2. Plot of the HOMO of complex **1**.

This observation is also confirmed by the failure of all the computational efforts to obtain any interaction of an incoming H<sub>2</sub> molecule with the nitrogen center.

Next, the mechanism of CO<sub>2</sub> hydrogenation to formate was studied using the computational methodology mentioned above, and the obtained reaction pathway is shown in Figure 3 and in Figure S.18 (Supporting Information). A preactivation step involving the removal of one carbonyl ligand from **1**, generating a free coordination site from the octahedral geometry, was at first evaluated. It was calculated that a free energy cost of +16.4 kcal mol<sup>-1</sup> is needed to obtain the pentacoordinate complex [Mn(PNP)(CO)<sub>2</sub>] (**2**), renamed as **A** as starting point in the reaction pathway, that can be considered as the active species in the catalytic cycle.

The availability of a free coordination site allows the coordination of incoming H<sub>2</sub> to give complex [Mn(η<sup>2</sup>-H<sub>2</sub>)(PNP)(CO)<sub>2</sub>] (**B**), with a free energy cost of +4.4 kcal mol<sup>-1</sup>. Such a contribution is mainly due to the disfavored entropic term, with a slightly exothermic enthalpic contribution of -2.7 kcal mol<sup>-1</sup>. The optimized structure of **B** shows a symmetric η<sup>2</sup>-coordination to the metal with Mn–H distance of 1.69 Å and a H–H distance elongated by ca. 0.1 Å compared to the value obtained for the free H<sub>2</sub> molecule. The coordination of H<sub>2</sub> to the metal caused the appearance of an active infrared mode at 3205 cm<sup>-1</sup> associated with the H–H bond stretching. In the following step, the η<sup>2</sup>-H<sub>2</sub> ligand undergoes activation by interaction with the external base DBU, that has a much stronger basic character than the N atom of the PNP ligand, as discussed above. The interaction between **B** and DBU allows the formation of an initial adduct **C** featuring a long N(DBU)–H(H<sub>2</sub>) distance of 2.26 Å with a free energy cost +7.8 kcal mol<sup>-1</sup>. The long N–H distance does not cause any significant elongation of the H–H bond. From **C**, the system evolves through the transition state TS<sub>C-D</sub> featuring an η<sup>1</sup>-coordination of the H<sub>2</sub> moiety to Mn and with the other hydrogen interacting with the DBU nitrogen (DBU–H distance 1.47 Å). The estimated free energy barrier to reach TS<sub>C-D</sub> is 6.2 kcal mol<sup>-1</sup>. The transition state nature has been confirmed by the detection of a single imaginary frequency at -550 cm<sup>-1</sup> associated with the formation of a DBU–(H<sup>δ+</sup>) and a Mn–(H<sup>δ-</sup>) bonds. Then, the reaction evolves to give a tight ion pair **D** with a free energy gain of -9.0 kcal mol<sup>-1</sup>. **D** exhibits an already formed Mn–H bond with a distance of 1.6 Å between the two atoms, for example shorter than the value found in the X-ray structure of [MnH(PN<sup>3</sup>P)(CO)<sub>2</sub>],<sup>[6]</sup> whereas the H–H separation becomes 1.4 Å. The complete separation of the ion pair to obtain the anionic hydride complex [MnH(PNP)(CO)<sub>2</sub>]<sup>-</sup> (**E**) was estimated to be endergonic by +10.6 kcal mol<sup>-1</sup>.

The calculated Wiberg bond indexes<sup>[22]</sup> for the Mn–H bond was 0.78, suggesting a localization of electron density that makes **E** a good nucleophile for an incoming electrophile such as CO<sub>2</sub>. The reaction of **E** with CO<sub>2</sub> leads then to complex **F**, featuring a κ<sup>1</sup>-H coordinated formate with a greatly elongated Mn–H distance of 1.86 Å and an already formed C–H bond at 1.19 Å. In (κ<sup>1</sup>-H)**F** the incoming CO<sub>2</sub> moiety is bent by an angle of 133°, far from the free linear geometry (180°). The formation of (κ<sup>1</sup>-H)**F** from **E** and CO<sub>2</sub> was evaluated to be exergonic by



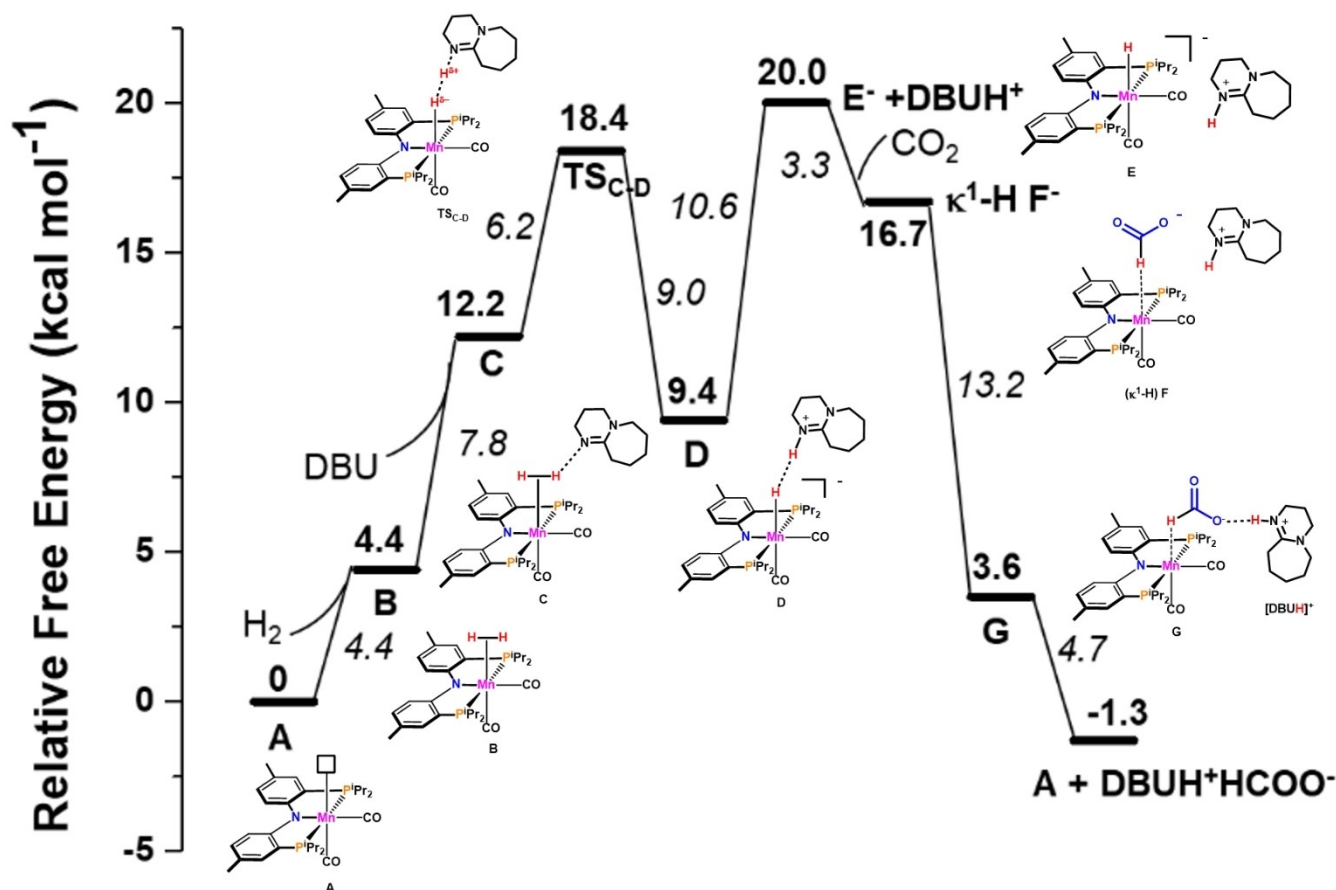


Figure 3. Free energy reaction pathway ( $\text{kcal mol}^{-1}$ ) for  $\text{CO}_2$  hydrogenation to formate in presence of DBU catalyzed by A.

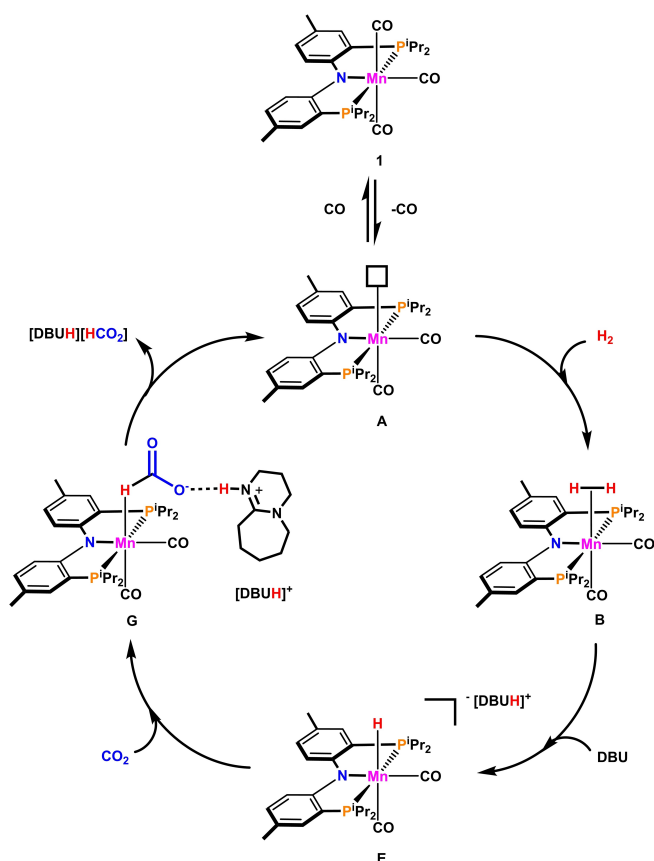
$-3.3 \text{ kcal mol}^{-1}$ . A similar interaction has also been proposed for other Mn-catalyzed  $\text{CO}_2$  hydrogenation processes,<sup>[6]</sup> and more recently by Lei and coworkers, in the presence of  $[\text{MnH}\{(\text{Ph}_2\text{PCH}_2\text{SiMe}_2)_2\text{NH}\}(\text{CO})_2]$ .<sup>[18]</sup> Although using different computational methodology, the analysis revealed a somewhat hindered process from the energetic (endergonic formation of the adduct) and structural points of view (short Mn–H distance still present in the first adduct). The slight endergonicity associated with the formation of a  $\kappa^1\text{-H}$  coordinated formate intermediate, starting from a Mn(I) hydride complex with similar PNP pincer ligands, was also observed by Moni and Mondal.<sup>[23]</sup>

Once F is obtained, the decooordination of the formate ligand to give back A may occur with or without prior isomerization from  $(\kappa^1\text{-H})\text{F}$  to  $(\kappa^1\text{-O})\text{F}$ . This step was described before in other Mn-catalyzed  $\text{CO}_2$  hydrogenation systems,<sup>[6,18,23]</sup> and is generally considered as a thermodynamic sink for the process. In our case, starting from  $(\kappa^1\text{-H})\text{F}$ , formate extrusion was estimated to be slightly endergonic by  $+0.87 \text{ kcal mol}^{-1}$ . This small contribution was also confirmed by the Wiberg indexes analysis for the Mn–H bond in  $(\kappa^1\text{-H})\text{F}$ , with a calculated value of 0.22 compared to the starting value of 0.78, suggesting the weakness of the Mn–H bonding after the interaction with  $\text{CO}_2$ . A more favorable free energy gain of  $-13.2 \text{ kcal mol}^{-1}$  was obtained by taking into account the  $[\text{DBUH}]^+$  cation, through the formation of adduct G with an interaction between the  $\text{O}^-$

atom of the coordinated formate and the H atom of the protonated DBUH<sup>+</sup>, leading to a more elongated Mn–H distance ( $1.97 \text{ \AA}$ ) and a shortened C–H distance ( $0.03 \text{ \AA}$ ). The complete decooordination step leading to  $[\text{DBUH}]^+[\text{HCO}_2]^-$  salt and A, closing the catalytic cycle, has a free energy gain of  $-4.7 \text{ kcal mol}^{-1}$ .

The  $(\kappa^1\text{-H})\text{F}$  to  $(\kappa^1\text{-O})\text{F}$  isomerization step was also calculated, and in agreement with previous results, the  $(\kappa^1\text{-O})\text{F}$  was found to be more stable by  $9.1 \text{ kcal mol}^{-1}$ . A free energy barrier associated to the isomerization was estimated to be  $6.9 \text{ kcal mol}^{-1}$ . Then, the system would evolve toward the complex  $(\kappa^1\text{-O})\text{F}$  with a free energy gain of  $-16 \text{ kcal mol}^{-1}$ . In any case, such a reaction route has been discharged in view of the more endergonic release of the formate ( $10 \text{ kcal mol}^{-1}$ ) compared to the same process from complex  $(\kappa^1\text{-H})\text{F}$ . In addition, the experimental observation of a positive effect of added Li salts on TONs, that was already demonstrated to stabilize  $(\kappa^1\text{-H})$  vs.  $(\kappa^1\text{-O})$  coordinated formate species in  $\text{CO}_2$  hydrogenation,<sup>[6,17]</sup> suggests that also in our case the  $(\kappa^1\text{-H})\text{F}$  species has a pivotal role in the catalytic cycle.

Based on these results, we propose the simplified catalytic cycle shown in Scheme 2. The total free energy for the entire reaction pathway was calculated as  $-1.3 \text{ kcal mol}^{-1}$ .



**Scheme 2.** Proposed simplified catalytic cycle for CO<sub>2</sub> hydrogenation to formate in the presence of precatalyst 1.

## Conclusions

In summary, it was shown that CO<sub>2</sub> hydrogenation to formate can be achieved in high yields and TONs = ca. 3800 in the presence of as low as 0.02 mol% of the neutral, coordinatively saturated tris(carbonyl) manganese pincer-type complex [Mn(PNP)(CO)<sub>3</sub>] (1), stabilized by the deprotonated form of bis(2-(diisopropylphosphino)-4-methylphenyl)amine (PNP), using DBU as base and LiOTf as Lewis acid additive, under mild reaction conditions (60 bar total pressure, 80 °C, 72 h). DFT calculations showed that a pentacoordinate active species such as [Mn(PNP)(CO)<sub>2</sub>] (2), can be generated by thermal decarboxylation and that this step requires 16.3 kcal mol<sup>-1</sup>. The hydrido complex [MnH(PNP)(CO)<sub>2</sub>]<sup>-</sup> (3) is then formed by intermolecular dihydrogen heterolytic cleavage assisted by DBU, instead of the expected intramolecular MLC-type mechanism involving the N donor atom of the PNP ligand, possibly due to the higher Lewis basicity of the DBU nitrogen atom. The highest barrier encountered along the reaction pathway is ca. 20 kcal mol<sup>-1</sup>, in line with the experimental reaction conditions. In our opinion, these results suggest that for CO<sub>2</sub> homogeneous hydrogenation in the presence of pincer-type complexes, the presence of possible non-MLC pathways should be carefully considered and evaluated.

## Experimental Section

**General Procedure for Carbon Dioxide Catalytic Hydrogenation.** In a typical experiment, the catalytic mixture containing solvent, catalyst, base and additive (if any) was prepared in a Schlenk tube under nitrogen and subsequently injected into a 40 mL magnetically stirred teflon-lined stainless steel autoclave built at CNR-ICCOM, kept under a nitrogen atmosphere. Then, the autoclave was pressurized with a H<sub>2</sub>/CO<sub>2</sub> gas mixture at the desired pressure, it was placed into an oil bath pre-heated to the desired temperature and left stirring at 500 rpm for the set reaction time. After the run, the autoclave was cooled to < 10 °C using an ice bath, the pressure was gently released and the reaction mixture was transferred into a round bottom flask. The autoclave beaker was thoroughly rinsed with H<sub>2</sub>O and the washings added to the rest of the mixture. The volume of the mixture was then gently reduced using a rotary evaporator at room temperature until a homogeneous mixture was obtained. DMF (300 μL) was added to the mixture as internal standard and the formate content was determined by integration of the corresponding <sup>1</sup>H NMR signal vs. DMF. D<sub>2</sub>O (ca. 0.7 mL) was added as deuterated solvent. All tests were repeated at least twice to check for reproducibility.

## Supporting Information

General methods and materials, selected NMR spectra and DFT calculation methods are available in the Supporting Information. The authors have cited additional references within the Supporting Information.<sup>[24–26]</sup>

## Acknowledgements

This research was funded by the European Union – NextGeneration EU from the Italian Ministry of Environment and Energy Security POR H2 AdP MMES/ENEA with involvement of CNR and RSE, PNRR – Mission 2, Component 2, Investment 3.5 “Ricerca e sviluppo sull’idrogeno”, CUP: B93 C22000630006. Mr. Carlo Bartoli (CNR-ICCOM) is gratefully thanked for building and servicing the steel autoclaves used in this study.

## Conflict of Interests

The authors declare no conflict of interest.

## Data Availability Statement

The data that support the findings of this study are available in the supplementary material of this article.

**Keywords:** CO<sub>2</sub> hydrogenation · Manganese · pincer complexes · formates · catalytic mechanisms

[1] <http://www.noaa.gov/news-release/carbon-dioxide-now-more-than-50-higher-than-pre-industrial-levels>.

[2] a) H. Onyeaka, O. C. Ekwebelem, *Int. J. Environ. Sci. Technol.* **2023**, *20*, 4635–4648; b) D. N. Gorbunov, M. V. Nenasheva, M. V. Terenina, Y. S.

- Kardasheva, S. V. Kardashev, E. R. Naranov, A. L. Bugaev, A. V. Soldatov, A. L. Maximov, E. A. Karakhanov, *Pet. Chem.* **2022**, *62*, 1–39; c) *CO<sub>2</sub> Hydrogenation Catalysis* (Ed. Y. Himeda), Wiley-VCH, Weinheim, **2021**; d) *Chemical Transformations of Carbon Dioxide* (Eds. X.-F. Wu, M. Beller), *Topics in Current Chemistry Collections*, Springer, Berlin, **2018**; e) M. Scott, B. Blas Molinos, C. Westhues, G. Franciò, W. Leitner, *ChemCatChem* **2017**, *10*, 1085–1093; f) M. Aresta, A. Dibenedetto, A. Angelini, *Chem. Rev.* **2014**, *114*, 1709–1742; g) M. Peters, B. Koehler, W. Kuckshinrichs, W. Leitner, P. Markewitz, T. E. Mueller, *ChemSusChem* **2011**, *4*, 1216–1240; h) E. E. Benson, C. P. Kubiak, A. J. Sathrum, J. M. Smieja, *Chem. Soc. Rev.* **2009**, *38*, 89–99; i) M. Aresta, A. Dibenedetto, *Dalton Trans.* **2007**, 2975–2992.
- [3] a) J. Hietala, A. Vuori, P. Johnsson, I. Pollari, W. Reutemann, H. Kieczka, *Formic Acid. Ullmann's Encyclopedia of Industrial Chemistry*, Wiley-VCH, Weinheim, **2000**; b) S. Chatterjee, I. Dutta, Y. Lum, Z. Lai, K.-W. Huang, *Energy Environ. Sci.* **2021**, *14*, 1194–1246.
- [4] R. E. Siegel, S. Pattanayak, L. A. Berben, *ACS Catal.* **2023**, *13*, 766–784.
- [5] a) K. Das, S. Waiba, A. Jana, B. Maji, *Chem. Soc. Rev.* **2022**, *51*, 4386–4464; b) S. E. Gulyaeva, S. E. Osipova, R. Buhaibeh, Y. Canac, J.-B. Sortais, D. A. Valyaev, *Coord. Chem. Rev.* **2022**, *458*, art. no. 214421; c) L. Gonsalvi, A. Guerriero, S. Kostera, in *CO<sub>2</sub> Hydrogenation Catalysis* (Ed. Y. Himeda), Wiley-VCH, Weinheim, **2021**, pp. 53–88; d) B. G. Reed-Berendt, K. Polidano, L. C. Morrill, *Org. Biomol. Chem.* **2019**, *17*, 1595–1607; e) P. Gandeepan, T. Müller, D. Zell, G. Cera, S. Warratz, L. Ackermann, *Chem. Rev.* **2019**, *119*, 2192–2452; f) T. Zell, R. Langer, *ChemCatChem* **2018**, *10*, 1930–1940; g) G. A. Filonenko, R. van Putten, E. J. M. Hensen, E. A. Pidko, *Chem. Soc. Rev.* **2018**, *47*, 1459–1483; h) F. Kallmeier, R. Kempe, *Angew. Chem. Int. Ed.* **2018**, *57*, 46–60; i) N. Gorgas, K. Kirchner, *Acc. Chem. Res.* **2018**, *51*, 1558–1569; j) A. Mukherjee, D. Milstein, *ACS Catal.* **2018**, *8*, 11435–11469; k) B. Maji, M. Barman, *Synthesis* **2017**, *49*, 3377–3393; l) M. Garbe, K. Junge, M. Beller, *Eur. J. Org. Chem.* **2017**, 4344–4362; m) D. A. Valyaev, G. Lavigne, N. Lugan, *Coord. Chem. Rev.* **2016**, *308*, 191–235; n) J. R. Carney, B. R. Dillon, S. P. Thomas, *Eur. J. Org. Chem.* **2016**, 3912–3929.
- [6] F. Bertini, M. Glatz, N. Gorgas, B. Stöger, M. Peruzzini, L. F. Veiros, K. Kirchner, L. Gonsalvi, *Chem. Sci.* **2017**, *8*, 5024–5029.
- [7] A. Dubey, L. Nencini, R. R. Fayzullin, C. Nervi, J. R. Khusnutdinova, *ACS Catal.* **2017**, *7*, 3864–3868.
- [8] A. Kumar, P. Daw, N. A. Espinosa-Jalapa, G. Leitus, L. J. W. Shimon, Y. Ben-David, D. Milstein, *Dalton Trans.* **2019**, *48*, 14580–14584.
- [9] K. Schlenker, E. G. Christensen, A. A. Zhanserkeev, G. R. McDonald, E. L. Yang, K. T. Lutz, R. P. Steele, R. T. VanderLinden, C. T. Saouma, *ACS Catal.* **2021**, *11*, 8358–8369.
- [10] C. M. Hert, J. B. Curley, S. P. Kelley, N. Hazari, W. H. Bernskoetter, *Organometallics* **2022**, *41*, 3332–3340.
- [11] S. Kostera, S. Weber, M. Peruzzini, L. F. Veiros, K. Kirchner, L. Gonsalvi, *Organometallics* **2021**, *40*, 1213–1220.
- [12] D. Wei, R. Sang, P. Sponholz, H. Junge, M. Beller, *Nat. Energy* **2022**, *7*, 438–447.
- [13] a) J. R. Khusnutdinova, D. Milstein, *Angew. Chem. Int. Ed.* **2015**, *54*, 12236–12273; b) M. R. Elsby, R. T. Baker, *Chem. Soc. Rev.* **2020**, *49*, 8933–8987.
- [14] A. Bruneau-Voisine, D. Wang, T. Roisnel, C. Darcel, J.-B. Sortais, *Catal. Commun.* **2017**, *92*, 1–4.
- [15] a) L. Fan, B. M. Foxman, O. V. Ozerov, *Organometallics* **2004**, *23*, 326–328; b) O. V. Ozerov, C. Guo, V. A. Papkov, B. M. Foxman, *J. Am. Chem. Soc.* **2004**, *126*, 4792–4793; c) L. Fan, L. Yang, C. Guo, B. M. Foxman, O. V. Ozerov, *Organometallics* **2004**, *23*, 4778–4787; d) O. V. Ozerov, C. Guo, L. Fan, B. M. Foxman, *Organometallics* **2004**, *23*, 5573–5580; e) J. J. Davidson, J. C. DeMott, C. Douvris, C. M. Fafard, N. Bhuvanesh, C.-H. Chen, D. E. Herbert, C.-I. Lee, B. J. McCulloch, B. M. Foxman, O. V. Ozerov, *Inorg. Chem.* **2015**, *54*, 2916–2935.
- [16] A. T. Radosevich, J. G. Melnick, S. A. Stoian, D. Bacciu, C.-H. Chen, B. M. Foxman, O. V. Ozerov, D. G. Nocera, *Inorg. Chem.* **2009**, *48*, 9214–9221.
- [17] W. H. Bernskoetter, N. Hazari, *Acc. Chem. Res.* **2017**, *50*, 1049–1058.
- [18] L. Zhang, M. Pu, M. Lei, *Dalton Trans.* **2021**, *50*, 7348–7355.
- [19] a) A. A. Kassie, P. Duan, M. B. Gray, K. Schmidt-Rohr, P. M. Woodward, C. R. Wade, *Organometallics* **2019**, *38*, 3419–3428; b) A. J. Hallett, R. A. Baber, A. G. Orpen, B. D. Ward, *Dalton Trans.* **2011**, *40*, 9276–9283; c) P. Datta, S. K. Sarkar, T. K. Mondal, A. K. Patra, C. Sinha, *J. Organomet. Chem.* **2009**, *694*, 4124–4133; d) D. J. Blumer, K. W. Barnett, T. L. Brown, *J. Organomet. Chem.* **1979**, *173*, 71–76.
- [20] Gaussian 16, Revision C.01, M. J. Frisch, G. W. Trucks, H. B. Schlegel, G. E. Scuseria, M. A. Robb, J. R. Cheeseman, G. Scalmani, V. Barone, G. A. Petersson, H. Nakatsuji, X. Li, M. Caricato, A. V. Marenich, J. Bloino, B. G. Janesko, R. Gomperts, B. Mennucci, H. P. Hratchian, J. V. Ortiz, A. F. Izmaylov, J. L. Sonnenberg, D. Williams-Young, F. Ding, F. Lipparini, F. Egidi, J. Goings, B. Peng, A. Petrone, T. Henderson, D. Ranasinghe, V. G. Zakrzewski, J. Gao, N. Rega, G. Zheng, W. Liang, M. Hada, M. Ehara, K. Toyota, R. Fukuda, J. Hasegawa, M. Ishida, T. Nakajima, Y. Honda, O. Kitao, H. Nakai, T. Vreven, K. Throssell, J. A. Montgomery, Jr., J. E. Peralta, F. Ogliaro, M. J. Bearpark, J. J. Heyd, E. N. Brothers, K. N. Kudin, V. N. Staroverov, T. A. Keith, R. Kobayashi, J. Normand, K. Raghavachari, A. P. Rendell, J. C. Burant, S. S. Iyengar, J. Tomasi, M. Cossi, J. M. Millam, M. Klene, C. Adamo, R. Cammi, J. W. Ochterski, R. L. Martin, K. Morokuma, O. Farkas, J. B. Foresman, D. J. Fox, Gaussian, Inc., Wallingford CT, **2016**.
- [21] C. Adamo, V. Barone, *J. Chem. Phys.* **1999**, *110*, 6158–6169.
- [22] K. B. Wiberg, *Tetrahedron* **1968**, *24*, 1083–1087.
- [23] S. Moni, B. Mondal, *Catalysts* **2023**, *13*, art. no. 592.
- [24] S. Grimme, S. Ehrlich, L. Goerigk, *J. Comb. Chem.* **2011**, *32*, 1456–1465.
- [25] M. Cossi, N. Rega, G. Scalmani, V. Barone, *J. Comput. Chem.* **2003**, *24*, 669–681.
- [26] M. Dolg, H. Stoll, H. Preuss, R. M. Pitzer, *J. Phys. Chem.* **1993**, *97*, 5852–5859.

Manuscript received: August 13, 2023

Accepted manuscript online: September 18, 2023

Version of record online: October 27, 2023